

# Searching for the Lightest Neutralino at Fixed Target Experiments

L. Borissov, J. M. Conrad, M. Shaevitz  
*Columbia University, New York, NY, 10027*  
 (December 2, 2024)

Most ongoing supersymmetry searches have concentrated on the high-energy frontier. High-intensity fixed target beam-lines, however, offer an opportunity to search for supersymmetric particles with long lifetimes and low cross-sections in regions complementary to the ones accessible to collider experiments. In this paper, we consider  $R$ -parity violating supersymmetry searches for the lightest neutralino and use the NuTeV experiment as an example for the experimental sensitivity which can be achieved.

## I. MOTIVATION

A review of supersymmetric models can be found in [1]. We consider models where the lightest neutralino ( $\tilde{\chi}_1^0$ ) is the Lightest Supersymmetric Particle (LSP). If the LSP is allowed to decay,  $R$ -parity violation ( $\mathcal{R}_p$ ) is required via the superpotential:

$$W_{\mathcal{R}_p} = \lambda_{ijk} L_i L_j \bar{E}_k + \lambda'_{ijk} L_i Q_j \bar{D}_k + \lambda''_{ijk} \bar{U}_i \bar{D}_j \bar{D}_k \quad (1)$$

where  $i, j$  and  $k$  are generation indices;  $L$  and  $Q$  are the lepton and quark  $SU(2)$  superfields;  $E, U$ , and  $D$  are the lepton and quark  $U(1)$  superfields and  $\lambda_{ijk}, \lambda'_{ijk}$ , and  $\lambda''_{ijk}$  are Yukawa-type couplings between the fields. This model is specified by the squark and slepton masses; mass terms for the gauginos at the electroweak scale ( $M_1, M_2$  and  $M_3$ ), the ratio of vacuum expectation values of the two neutral Higgses ( $\tan\beta$ ); a mass term mixing the two Higgs doublets ( $\mu$ ) and the values of the  $\lambda$ -couplings.

In the Minimal Supersymmetric Standard Model (MSSM), unification is imposed at the GUT-scale, which leads to the relation:

$$M_1 = \frac{5}{3} \tan^2 \theta_W M_2 \approx 0.5 M_2 \quad (2)$$

where  $\theta_W$  is the weak mixing angle at the electroweak scale. Assuming Eq. (2), current LEP data give  $m_{\tilde{\chi}_1^0} > 32.3$  GeV [9,22]. In the  $\mathcal{R}_p$  scenario, collider experiments require the  $\tilde{\chi}_1^0$  to decay inside the detector. This leads to very low sensitivity for a long lifetime low mass  $\tilde{\chi}_1^0$  [9]. Moreover, if the GUT-scale unification requirement (2) is not assumed, such neutralinos can be produced in observable quantities in lifetime regions inaccessible to collider experiments. Coverage in these regions can be achieved by a detector far from the collision vertex, provided there is enough luminosity and cross-section for neutralino production.

In the following analysis, we present an example of the experimental sensitivity for  $\mathcal{R}_p$  SUSY with lepton number violation ( $\lambda_{ijk} > 0$ ) of a high-intensity fixed target experiment. We are interested in very low mass  $\tilde{\chi}_1^0$ , so we do not require the relation given in Eq. (2), leaving  $M_1$  and  $M_2$  to be free parameters. However, bounds from the invisible decay of the  $Z^0$  necessitate that  $M_1$  is very small, so that the  $\tilde{\chi}_1^0$  is mostly bino and only its Higgsino admixture couples to the  $Z^0$  [8,12]. Thus we work in the framework of phenomenologically motivated  $\mathcal{R}_p$  unconstrained MSSM (uMSSM). However our model is very close to the MSSM except for GUT-scale unification and  $R$ -parity conservation. Motivation for  $\mathcal{R}_p$  models can be found in Refs. [4–7], while motivation for very low mass  $\tilde{\chi}_1^0$  is presented in Ref. [16].

## II. AN EXAMPLE: NUTEV

The NuTeV experiment (E815) [17–19] took data during the 1996-1997 fixed target run at Fermilab. NuTeV was designed to perform precision measurements of Standard Model parameters through deep inelastic neutrino-nucleon scattering. These measurements provide competitive and in many cases unique tests of the present-day understanding of the Standard Model, complementary to direct measurements from collider experiments.

During the run, 800 GeV protons from the Tevatron are incident upon a 20.5 cm BeO target at a 7.8 mrad angle. A total of  $2.86 \times 10^{18}$  protons on target were recorded during the live time of the detector. The protons interact and produce a secondary beam of pions, kaons and other hadrons. A system of quadrupole magnets – the Sign-Selected Quadrupole Train (SSQT) picks out secondaries of the correct sign and dumps wrong sign particles. After focusing, the pions and kaons enter a 541 m decay pipe, where they decay in flight with dominant modes  $\pi \rightarrow \nu_\mu \mu$ ,  $K \rightarrow \nu_\mu \mu$  and  $K \rightarrow \pi^0 \nu_\mu \mu$ . Approximately 3% of the mesons decay in the pipe, the rest are dumped in 6 m of aluminum and steel. The muons range out in 241 m of steel shielding and 582 m of earth berm. The resulting beam is a nearly pure neutrino beam with less than 0.2% contamination; it exhibits a dichromatic spectrum corresponding to the superposition of  $\pi$  and  $K$  decay distributions.

The NuTeV detector is situated 1.5 km downstream from the target. The calorimeter consists of 168 steel plates ( $3 \text{ m} \times 3 \text{ m} \times 5.1 \text{ cm}$ ), 84 liquid scintillation counters (every 10.2 cm of steel) and 42 drift chambers (every

20.4 cm of steel) followed by a 15 kG toroidal spectrometer. Upstream of the calorimeter is a 35 m decay region consisting of three large helium bags and six drift chambers (Fig. 1). The decay channel is shielded by an upstream veto wall.

### A. Production and decay

At the NuTeV target,  $\tilde{\chi}_1^0$ 's can be pair-produced in the  $s$ -channel via a  $Z$ , or in the  $t$ -channel through an exchange of a squark (Fig. 2). If the squark mass is sufficiently small, production can be enhanced. For our estimates, however, we have chosen to work with sfermion masses of the order of 800 GeV, conservatively above present experimental bounds [8]. Thus the only relevant production parameters are  $M_1, M_2, \mu$ , and  $\tan\beta$ . Production is insensitive to  $M_3$ , which is responsible for the gluino mass.

NuTeV uses a high intensity proton beam, but its center-of-mass energy ( $\sqrt{s} \approx 39$  GeV) is low compared to collider experiments. This, however, simplifies the search, since the only relevant mode at this energy is neutralino pair production.

In  $\mathcal{R}_p$  MSSM, the  $\tilde{\chi}_1^0$  decays leptonically according to the diagrams shown in Fig. 3. It is often assumed that only one of the  $LLE$  operators in Eq. (1) has a sizeable  $\lambda_{ijk}$  coupling, in order to explain the smallness of  $L$ -violating terms in the renormalizable Lagrangian required by present limits [11]. This is also the case of greatest experimental interest. For example, if  $\lambda_{122}$  is dominant, the  $\tilde{\chi}_1^0$  decays into  $\nu_e \mu^+ \mu^-$  and  $\nu_\mu e^\pm \mu^\mp$  with branching ratios of approximately 50% in each of the two channels [9]. The final state of two leptons and missing energy can be easily detected by an experiment such as NuTeV. The other extreme case,  $\lambda_{133}$  dominant, leads to decays mainly into taus and electrons. The efficiencies for the other  $\lambda_{ijk}$  couplings lie between these two cases.

The partial width for the  $\tilde{\chi}_1^0$  decaying into  $\nu ll'$  is of the typical form for a fermion three-body decay [11]:

$$\Gamma_{\tilde{\chi}_1^0} = K^2 \frac{G_F^2 m_{\tilde{\chi}_1^0}^5}{192 \pi^3} \quad (3)$$

where  $K$  is an effective four-fermion coupling in  $\tilde{\chi}_1^0$  decays (Fig. 3) proportional to the  $\tilde{\chi}_1^0 f\bar{f}$  coupling and the  $\mathcal{R}_p$  coupling  $\lambda_{ijk}$ . For a large region of SUSY parameter space

$$K \sim 0.1 \left( \frac{100 \text{ GeV}}{m_{\tilde{f}}} \right)^2 \lambda_{ijk} \quad (4)$$

where  $m_{\tilde{f}}$  is the mass of the virtual selectron or sneutrino exchanged [12].

Upper bounds on  $\lambda_{ijk}$  and can be found in [13,11]. The ones pertinent to our case of study are:

$$\lambda_{122} < 0.049 \times \frac{m_{\tilde{e}_R}}{100 \text{ GeV}} \quad (5)$$

$$\lambda_{133} < 0.006 \times \sqrt{\frac{m_{\tilde{\tau}}}{100 \text{ GeV}}} \quad (6)$$

which come from current universality requirements and limits on  $\nu_e$  mass [13].

Eq. (4) can be rewritten in terms of the average decay length in the lab frame:

$$l = 0.3(\beta\gamma) \left( \frac{m_{\tilde{f}}}{100 \text{ GeV}/c^2} \right)^4 \left( \frac{1 \text{ GeV}/c^2}{m_{\tilde{\chi}_1^0}} \right)^5 \frac{1}{\lambda^2} \quad (7)$$

### B. Predictions for the NuTeV experiment

The expected number of  $\tilde{\chi}_1^0$  decays detectedable by NuTeV is the product of the number  $\tilde{\chi}_1^0$ 's produced at the target passing through the detector and the probability that any of them actually decays in the He decay region (Fig. 1).

$$N_{evt} = \left( N_p d N_A \rho_{BeO} \frac{d\sigma}{d\Omega} d\Omega \right) \times \frac{(1 - e^{-\Delta z/l})}{e^{z/l}} \quad (8)$$

where  $N_p = 2.8 \times 10^{18}$  is the the number of protons on target,  $d$  is the length of the BeO target,  $\rho_{BeO} = 2.7 \text{ g/cm}^3$  is the target mass density,  $N_A$  is Avogadro's number;  $d\sigma/d\Omega$  is the differential production cross-section in the center-of-mass reference frame of the pair-production,  $d\Omega \approx 1.68 \times 10^{-3} \text{ rad}$  is the solid angle subtended by the detector in that reference frame;  $z$  is the distance between the target and the decay region,  $\Delta z$  is the length of the decay region and  $l = \gamma c\tau$  is the  $\tilde{\chi}_1^0$  decay length in the lab frame. For the NuTeV specifications, equation (8) gives:

$$N_{evt} \approx \left( 2.4 \times 10^{14} \text{ mb}^{-1} \frac{d\sigma}{d\Omega} \right) \times \frac{1 - e^{-\frac{3.5 \times 10^3 \text{ cm}}{l}}}{e^{\frac{1.5 \times 10^5 \text{ cm}}{l}}} \quad (9)$$

From Eq. (9), we make a contour plot of the expected number of observable  $\tilde{\chi}_1^0$  decays versus  $d\sigma/d\Omega$  and  $l$  as shown in Fig. 4. Since the expected signal is small, we use a Feldman and Cousins approach for the analysis [20]. The confidence level contours obtained are shown on Fig. 4. The uncertainty in  $\lambda_{ijk}$ , the sfermion mass and the  $\tilde{\chi}_1^0$  mass is conveniently folded into the  $\tilde{\chi}_1^0$  decay length  $l$ . Furthermore, we can use the fact that each of the contours has a minimum at  $l \approx 1.5 \times 10^5 \text{ cm}$  to set a conservative limit, independent of the Yukawa couplings and the sfermion mass by selecting the differential cross-section values at the minimum and using them to draw out exclusion regions in uMSSM space as shown on Fig. 5.

We perform a scan of uMSSM parameter space for  $M_1 = 1, 10 \text{ GeV}/c^2$ ,  $M_2 = 0, \dots, 200 \text{ GeV}/c^2$ ,  $\mu = -400, \dots, 400 \text{ GeV}/c^2$  and  $\tan\beta = 1.5, \dots, 40$ . We set  $m_{\tilde{f}} \approx 800 \text{ GeV}/c^2$  and  $M_3 = 1 \text{ TeV}$  [14,15].

The requirement that  $M_1$  is small, i.e.  $\tilde{\chi}_1^0$  is mostly bino ( $\tilde{B}$ ), allows us to obtain a bound on the  $\tilde{\chi}_1^0$  mass

independent of the Yukawa couplings or uMSSM parameters other than  $\tan\beta$  as shown on Fig. 6.

### III. CONCLUSIONS

The work presented here is an attempt to motivate  $R_p$  searches at fixed target experiments, since collider experiments run into sensitivity problems at low energy [8,9]. We argue that NuTeV and similar fixed target experiments, such as KTeV, may be in a unique position to complement collider searches. If supersymmetry exists at low energy, experiments like NuTeV, with good control over the production and decay backgrounds [21], could possibly make a discovery even at the few-event level.

### IV. ACKNOWLEDGEMENTS

We would like to thank to C. Quigg, J. Lykken, M. Carena, V. Barger, P. Nienaber and the NuTeV collaboration. This research was supported by the U.S. Department of Energy and the National Science Foundation.

[21] J. A. Formaggio *et al.*, hep-ex/9912062.

[22] ALEPH collaboration, preprint ALEPH 99-011, CONF 99-006

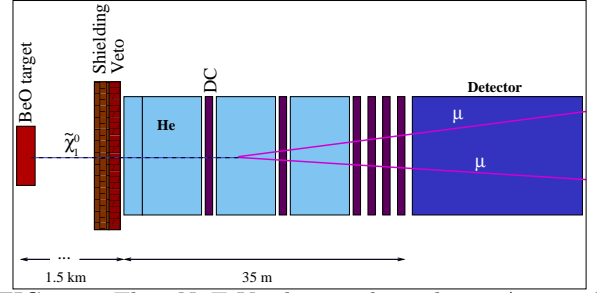


FIG. 1. The NuTeV decay channel. A possible  $\tilde{\chi}_1^0 \rightarrow \nu_e \mu^+ \mu^-$  decay is shown as seen by the detector.

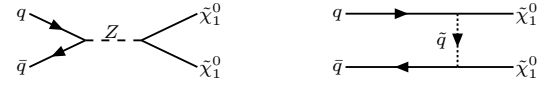


FIG. 2. Neutralino pair production mechanisms.

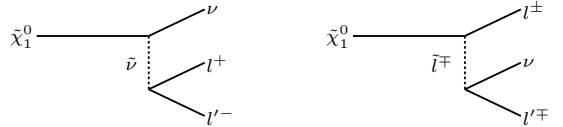


FIG. 3.  $\tilde{R}_p \tilde{\chi}_1^0$  decay mechanisms.

- 
- [1] S.P. Martin, hep-ph/9709356.
  - [2] V. Barger *et al.*, Phys. Rev. **D50**, 4299 (1994) hep-ph/9405245.
  - [3] H. Dreiner, Pramana **51**, 123 (1998).
  - [4] R.N. Mohapatra, *Maryland Univ. College Park - 86-185 (86,REC.AUG.) 17p*.
  - [5] S. Dimopoulos and L.J. Hall, Phys. Lett. **196B**, 135 (1987).
  - [6] W. Fischler *et al.*, Phys. Lett. **B258**, 45 (1991).
  - [7] L.E. Ibanez and G.G. Ross, Nucl. Phys. **B368**, 3 (1992).
  - [8] C. Caso *et al.*, Eur. Phys. J. **C3**, 1 (1998) Sect. 12.
  - [9] P. Abreu *et al.* [DELPHI Collaboration], CERN-EP-99-049.
  - [10] B. Allanach *et al.*, hep-ph/9906224.
  - [11] V. Barger, G.F. Giudice and T. Han, Phys. Rev. **D40**, 2987 (1989).
  - [12] H.E. Haber and G.L. Kane, Phys. Rept. **117**, 75 (1985).
  - [13] B.C. Allanach *et al.*, hep-ph/9906209.
  - [14] S. Mrenna, Comput. Phys. Commun. **101**, 232 (1997) hep-ph/9609360.
  - [15] T. Sjostrand, hep-ph/9508391.
  - [16] D. Choudhury, H. Dreiner, P. Richardson and S. Sarkar, hep-ph/9911365.
  - [17] D. A. Harris *et al.* [Nutev Collaboration], hep-ex/9908056.
  - [18] J. Conrad *et al.*, Rev. Mod. Phys **70**, 4 (1998).
  - [19] J. Yu *et al.* [Nutev Collaboration], FERMILAB-TN-2040.
  - [20] G. J. Feldman and R. D. Cousins, Phys. Rev. **D57**, 3873 (1998)

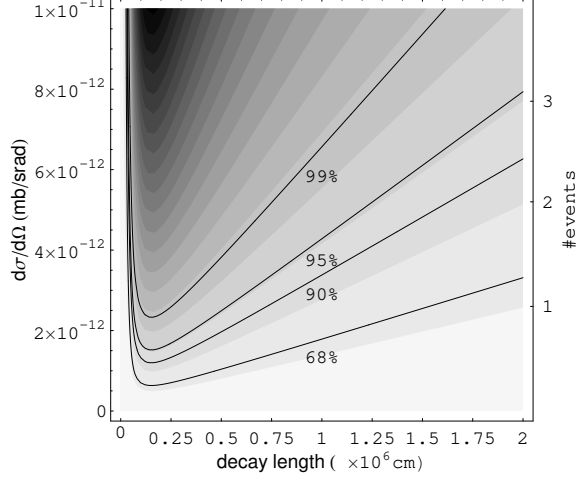


FIG. 4. Contour plots of  $\tilde{\chi}_1^0$  pair-production differential cross-section seen by the NuTeV detector versus  $\tilde{\chi}_1^0$  decay length in the lab frame. The colored contours represent the number of  $\tilde{\chi}_1^0$  decays occurring inside the detector assuming perfect detector efficiency. The four confidence level contours represent exclusion regions (above the contours) following a Feldman and Cousins approach and conservatively assuming 0 signal events and 0 background [20].

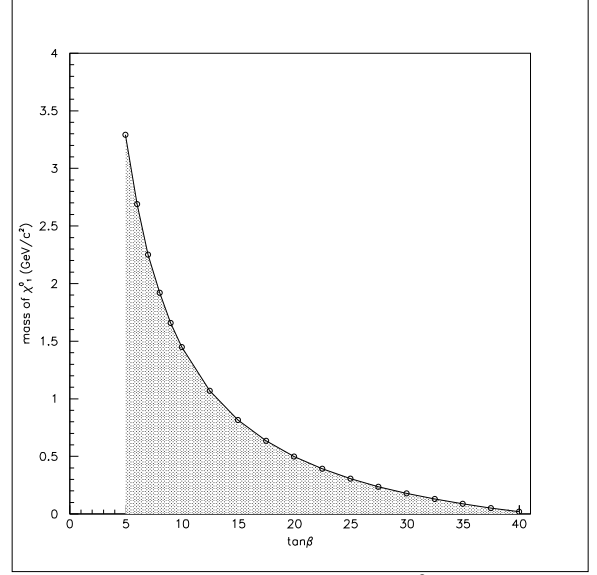


FIG. 6. 95% C.L. exclusion region for  $\tilde{\chi}_1^0$  mass as a function of  $\tan\beta$  for small  $M_1$  (here  $M_1 \ll 100 \text{ GeV}/c^2$ ).

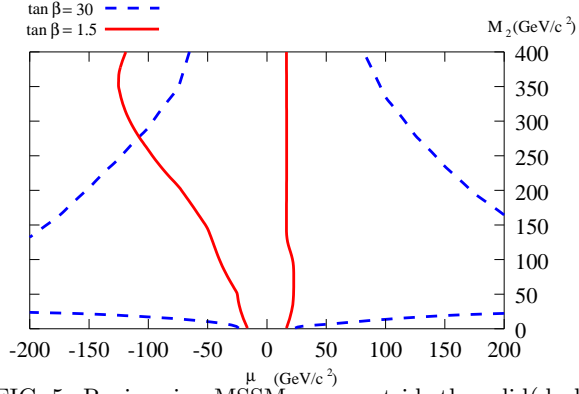


FIG. 5. Regions in uMSSM space outside the solid(dashed) lines are excluded for small(large)  $\tan\beta$  at  $M_1 = 1 \text{ GeV}/c^2$ .